Title
DESIGN OF STRONG, DUCTILE, HSLA, AND DUAL PHASE STEELS

Author
Thomas, G.

Publication Date
1986

Lawrence Berkeley Laboratory
UNIVERSITY OF CALIFORNIA

Materials & Molecular Research Division

Presented at the First Indo-US Workshop on Iron and Technology, Ranchi, India, January 6-9, 1986

DESIGN OF STRONG, DUCTILE, HSLA, AND DUAL PHASE STEELS

G. Thomas

January 1986

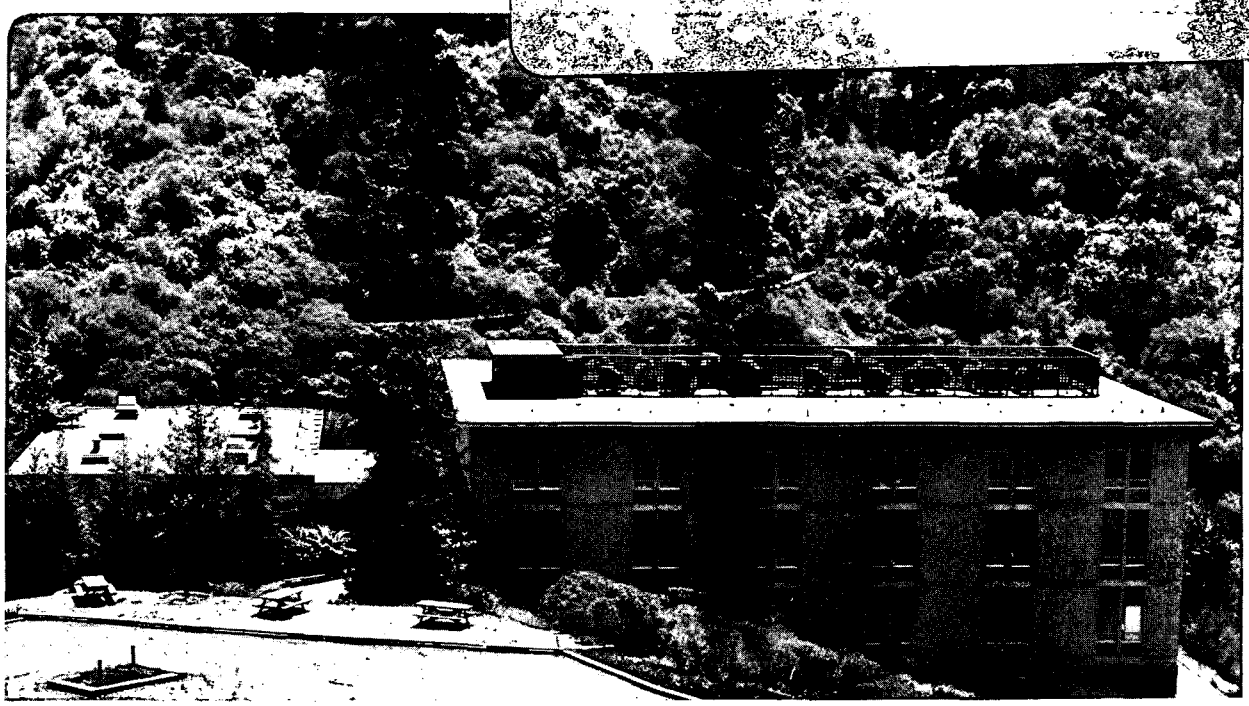

Prepared for the U.S. Department of Energy under Contract DE-AC03-76SF00098

DISCLAIMER

FIRST INDO-US WORKSHOP ON IRON & STEEL TECHNOLOGY

RANCHI, INDIA, JANUARY 6-9, 1986

DESIGN OF STRONG, DUCTILE, HSLA AND DUAL PHASE STEELS

Gareth Thomas

Professor, Department of Materials Science and Mineral Engineering

University of California

Berkeley, CA 94720

and

Scientific Director, National Center for Electron Microscopy

Materials and Molecular Research Division

Lawrence Berkeley Laboratory

Berkeley, CA 94720

USA

ABSTRACT

This paper summarises our alloy design programmes at Berkeley which utilise the concept of two-phase steels as a means of optimising these mutually exclusive properties. The underlying principle here is to design composite microstructures whereby the advantages of the second phase are optimised while the less desirable features of this phase are simultaneously mitigated by the presence of the other constituent phase. The size, distribution, shape and volume fraction of the second phase critically control the mechanical properties, especially fracture and fatigue of the dual phase systems. As a consequence, these structures offer a degree of metallurgical flexibility that is absent in single phase structures or in many precipitation strengthened systems, for attaining optimum sets of mechanical properties.

Examples are presented here of martensite/austenite (~2-5%) mixtures designed for optimum combinations of high strength, toughness, and wear properties in medium carbon steels, e.g., for mining and agricultural applications, and martensite/ferrite (~80%) structure for high strength, cold formability and improved low temperature ductility in low carbon steels. Applications to sheet, line pipe rods and wires will be demonstrated for the latter class of steels.

1. INTRODUCTION

There are current needs to optimise and conserve raw materials and energy, such that physical metallurgists and engineers are challenged to improve the mechanical properties of engineering alloys, in particular steels, and also to minimise high capital costs of new processing facilities. The major difficulty in optimising strength, toughness, and ductility in steels comes from the fact that strength is usually inversely related to toughness and ductility; the increase in the former is achieved at the expense of the latter and vice versa. This is true in the majority of cases when relatively inexpensive alloying and processing are sought for practical alloy development. This concept has been the basis for the alloy design programme for nearly two decades now at Berkeley, a programme which optimises ranges of mechanical properties through the characterisation and subsequent manipulation of the microstructure, chemical composition and processing. Three different classes of steels have been utilized in the programme, representing three of some of the most important uses of steel in industry today:

i) Structural steels as used in tough structures, mining and industries, and in defense applications.

ii) Steels used in the transportation industries, and line-pipe.

iii) Steels used as bars, rods, and drawn to high strength wires.

These categories require high-strength for load bearing, and high toughness and ductility to resist the propagation of cracks through the material and to ensure good formability. For mining and agricultural applications, wear and corrosion resistance are

significant properties also.

As schematically shown in fig. 1, conventional manipulation of mechanical properties through microstructural control has shown that high strength and high toughness are often conflicting requirements, as an increase in strength is often accompanied by a reduction in the ductility and fracture toughness. Typical microstructural effects that show this trend are solute strengthening, precipitation hardening and dislocation hardening. Nevertheless, two methods of microstructural control are available that can result in an increase in both properties--grain refinement and phase transformation through heat treatment. The principles of composites (viz mixing ductile and hard, tough phases with coherent interfaces) have formed the basis for the alloy design programmes we have developed and are based on the following scheme. a) medium carbon HSLA steels, exhibiting high strength and toughness as a result of a refined microstructure that is a composite of a strong, tough martensitic phase (major phase) and a softer, tough austenite phase; b) low carbon, "dual phase" steels, designed for high cold formability having a composite microstructure of ferrite (major phase) and martensite (or bainite).

2. STRUCTURE - PROPERTY RELATIONS

A. Strong, Tough, Wear-Resistant Medium Carbon HSLA Steels.

A systematic study of the relation between martensite microstructures and mechanical properties utilising a series of Fe-C-X high purity, vacuum-melted experimental alloys (where X is the substitutional solute) has been under way at Berkeley since 1964 (see Rao and Thomas [1], Thomas [2-4] for reviews. Optimisation of properties

through minimum alloying and processing routes has been achieved by controlling the austenite to martensite reaction so as to produce a refined packet martensite containing laths of a high density of dislocations, uniformly distributed, in a fine-grained microstructure [2], and where each lath is surrounded by a stable austenite film. The dislocations are a necessary component for both strength and toughness. Whether twinned or dislocated slip martensite occurs is determined mainly by the composition of the steel, in particular the carbon content through its effect in the transformation start temperature, Ms, a low MS means twinned plate martensite, which tends to be brittle and should be avoided. Thus the composition must be regulated to maintain Ms>200°C; this sets the carbon limit to about 0.3wt%. This microstructure which results in optimum mechanical properties, is a duplex austenite-martensite structure in which martensite laths are surrounded by thin films of retained austenite and can only be resolved by transmission electron microscopy (fig. 2). These steels have been designated "Quatough" and contain Cr(1-12) MN(1-2) and C(0.2-0.4)wt.%. The higher Cr ranges provide excellent corrosion resistance at high strength levels.

The excellent combinations of strength and toughness exhibited by the Quatough steels can be seen even in the untempered condition. Table 1 and figs. 3,4 shows typical data. Tempering in the 300-400°C temperature range leads to tempered martensite embrittlement (TME), and the drop in toughness is associated with the decomposition of the retained austenite to interlath carbides [5-7]. Recent studies [5,6,7] have shown that the retained austenite is remarkably stable, the activation energy for austenite decomposition being ~ 43 kcal/mole.

However the way in which austenite stabilisation occurs is not uniquely known. In an attempt to clarify the importance of chemical stabilisation of the austenite, the local chemical compostion of the region adjacent to the austenite/martensite interface has been examined. Using tranmission electron microscopy (lattice imaging and convergent beam microdiffraction), and atom-probe spectroscopy, it has been possible to show that the austentite is substantially enriched in carbon with large peak in the carbon concentration found at the austenite/martensite interface even in the as-quenched condition. Figure 5 shows a summary of these techniques. The results show carbon depletion has occurred in the martensite matrix, although the distribution is non-unifrom due to autotempering, carbon enrichment in austenite, and at the austenite-martensite interface which is considerable. Although chemical stabilisation is obviously a factor in austenite stabilisation, mechanical stabilisation and the size effect [8], i.e., the retained austenite exists as thin films 50-250 A thick, also play important roles.

In addition to the microscopy experiments described above, in-situ fracture studies have been performed using thin foils of quenched, and quenched and tempered steels, in a high voltage electron microscope equipped with a tensile stage [7]. Fracture appears to occur exclusively within the martensite laths. In the tough condition, fracture is preceded by localised slip, work-hardening, thinning down (necking) and hole formation. Packets of laths unfavoraby oriented, do not participate in fracture initiation. In the tempered condition, slip and failure depends on carbide morphology. It is suggested that the fracture process depends primarily on the plastic deformation

characteristics of the martensite laths, which in turn are affected by the microstructure. This is shown schematically in fig. 6.

With the increasing potential application for structural steels in a "dynamic" structure (where the resistance to fatigue plays an important role), such as machinery in the mining industry, the fatigue properties of the experimental quatough steels have been analyzed to avoid the possibility that an increase in toughness is obtained at the expense of fatigue properties. The results have shown that variations in fracture toughness (K_{IC}) from 65 $MPam^{1/2}$ to 198 $MPam^{1/2}$ (induced by varying Mn alloying element and by 200°C tempering), appear to have little effect on the "mid-range" of crack growth rates exceeding 5 x 10^{-6} nim/ cycles. In addition, the experimental steels have better fatigue resistance in the medium crack growth range than commercial steels AISI 4340 and 300M for the same heat-treatment conditions such as in the as-quenched or 200°C tempered states, as shown in fig. 7.

Many of the uses of structural steels require not only good strength-toughness characteristics, but also good wear-corrosion-resistance. As part of the alloy design programme, both sliding and abrasive wear behavior have been examined and measured for the quatough steels [9-11]. The results show that the duplex martensite/austenite microstructure of these steels exhibits good wear-resistance in both categories of wear, and are superior to many, commercial alloys that are described as wear-resistant alloys (see fig. 8). Sliding wear behavior was found to be beneficially affected by tensile strength, hardness, fracture toughness, and grain-refinement, whereas abrasive wear was found to be postively affected by only the first two factors. More recently, the sliding wear

behavior of these steels has been further enhanced by laser surface hardening. Using a 500 watt, continuous CO_2 laser, localised, rapid heating and quenching can be confined to the surface of the alloys, producing a hard, grain-refined microstructure to depths of 500 microns and hence, a two fold increase in wear resistance. In addition to these studies, a more fundamental study is continuing into the mechanisms of wear. The results suggest for several iron-based materials, tested in air, wear particles are formed by crack initiation and propagation along the boundary of dislocation cells present in a deformed region found adjacent to the wear surface. Oxidation than occurs during separation of the platelet from the parent material. Consequently, materials with a fine-scale microstructure and a high yield strength, in the absence of large undeformable particles, appear to be the most wear resistant.

Finally, the corrosion properties of some of the experimental steels have been examined and compared to commercial alloys as well as the dual phase steels discussed in the following section. Some data are shown in Table II. The 4wt% chromium steels give good corrosion resistance as the table shows, and have greater corrosion resistance than 4340, a structural steel of similar properties.

B. Dual-Phase, Low-Carbon Steels. During the past several years, dual-phase ferrite-martensite steels, especially for flat products have received increasing attention [12-14], as having high strength and ductility combined with excellent cold formability. The strengthening principle of the dual-phase structure involves the incorporation of inherently strong martensite, as the load-carrying constituent, in a soft, ferrite matrix, which supplies the system with

the essential ductility. Thus, these alloys can be considered equivalent to fibre composites, with the advantage of producing coherent phases by solid-state phase transformation (fig. 9). The basic physical metallurgy and alloy design principles followed at Berkeley have been described in detail in several recent papers, [15,16] and will not be repeated here. However, it is emphasized that the properties of dual-phase steels are largely dependent upon these factors:

(i) morphology--size, shape and distribution of both the ferrite and martensite

(ii) the microstructure, and hence the properties of the phases, and

(iii) the volume fraction of martensite (or bainite).

Of these factors, morphology plays the most important role in controlling ductility [17] and fatigue [18-23]. It has been shown that a coarse dual-phase structure has very poor tensile elongation ductility. This is due to cleavage crack initiation and propagation within the ferrite matrix where the maximum stress concentration takes place. However, when the microstructure is refined, the degree of stress concentration decreases, and fracture is initiated by void nucleation and growth around the ferrite/martensite interfaces. These voids, once initiated, propagate within the ferrite matrix without fracture occurring within the martensite. The effect of microstructure on the fatigue behavior of metals is not unambiguously understood. (See ref. 19 for review). For example, in the realm of low cycle fatigue (LCF) it is desirable to disperse slip to prevent crack initiation. This can be accomplished by increasing the strain

hardening capacity of the material. On the other hand, treatments which increase strain hardening to not appear to enhance crack propagation behavior and in fact there appears to be a growing body of information that indicates slip concentration is associated with improved fatigue crack propagation (FCP) properties.

Many microstructural effects, particularly at near-threshold levels, can be linked to a prominant role of crack closure, i.e., to extrinsic mechanisms. Of these, grain size, precipitate type and distibution, slip characteristics and the proportion and morphology of the two phases, appear to be important variables.[20--23] In many instances, optimizing these variables for maximum fatigue resistance can have the opposite effect on other mechanical properties, such as toughness, ductility and resistance to crack initiation. For example, increasing grain size can increase ΔK_{TH} values yet this generally reduces fracture toughness and the initiation-controlled fatigue limit. Fatigue crack propagation behavior in dual-phase steels provides an illustrative example of some of these effects, since the microstructures provide an excellent system to improve crack growth resistance through the generation of tortuous crack paths by deflection at interfaces, leading to enhanced roughness-induced closure [19, 22, 23]. Recent studies have shown that by modifying the proportion and morphology of the ferrite and martensite phases through intercritical heat treatment (fig. 10) increases in the ΔK_{TH} value by up to a factor of two can be readily obtained without loss in strength (fig. 11). Such marked increases in crack growth resistance, are associated with measured increases in closure and can be attributed directly to the production of meandering crack paths (fig. 12).

The benefits of this approach in dual-phase steels are that very high thresholds are obtained without losing tensile strength, and hence without compromising crack initiation resistance. Dual phase steels of simple composition provide the largest fatigue threshold - yield strengths ever reported (fig. 13).[23]

The tensile strengths on the other hand, appears to be less sensitive to morphology, and depends approximately, and in an empirical fashion, on the "law of mixtures" given below,

$$\sigma_c = \sigma_M V_M + \sigma_\alpha (1 - V_M)$$

Eq. 1

where σ_M and σ_α are the strengths of martensite and ferrite respectively, and V_M and $(1 - V_M$ are their corresponding volume fractions. In general, there is a linear increase in strength with increase in volume fraction of martensite. However, in some alloy systems which contain carbide-forming elements such as Nb and Mo, the strength decreases or remains constant[24] with increasing martensite volume fraction; this represents an anomaly in the usual "law of mixtures" behavior as shown in figs. 14, 15. If the volume fraction of martensite is increased by raising the annealing temperature within the $(\alpha+\gamma)$ field, then two ways are possible wherein the strength of th.e steel can be reduced. The first is by a decrease in the carbon content of the ferrite, which leads to a decrease in the density of carbide precipitation in the ferrite[25] and the second is by a decrease

in the carbon content of the martensite, thus lowering its strength. The overall effect, which depends on the relative magnitude of thse factors, can result in a negative slope in the "law-of-mixtures" equation (Eq. 1), if the strength of the ferrite changes significantly (fig. 15). Thus, the complex interactions of parameters such as morphology, properties and volume fraction of constituent phases must all be controlled when designing dual-phase alloys. When this is achieved, excellent mechanical properties can be realized, with high strengths attainable for low carbon (0.1% or less) alloys. Moreover, the alloy compositions are quite simple, with no need for microalloying elements, and are therefore inexpensive. Also by controlling the composition, considerable flexibility in the processing is attainable [24].

Several ranges of simple alloys have been developed in the alloy design program, starting with a simple Fe/Si/C alloy, which has the fibrous structure shown in figs. 9, 10 and has excellent properties (fig. 9). Although interest in dual-phase steels has been generated largely by the recent fuel crisis and its impact on the need for weight savings in transportation systems, i.e., for flat sheet products, the potential application for dual-phase alloys are broad indeed. These alloys form a new class of strong, ductile steels for applications requiring tensile strength levels of ~100 ksi for sheet, (e.g.pipeline),rods, bars, etc. and up to 400 ksi for tensile wire. The latter properties can be obtained by cold wire drawing without the necessity for intermediate patenting heat treatments [26, 27] (see fig. 16). Strengths up to 400 ksi are indeed remarkable for such simple steels with less than 0.1wt% carbon. More details have been

summarised in ref. 28, which also describes the on-line rolling method for producing dual phase products (fig. 17), without further intercritical annealing.

Steels used for pipeline must have high strength as well as high toughness (low ductile-to-brittle transition temperature). The alloy design principle for pipeline application is that high toughness can be obtained primarily by grain size control, while maintaining a dual-phase structure to simultaneously obtain high strength. Controlled rolling of a Fe/1.5Mn/0.06C alloy, followed by direct quenching produces a duplex microstructure in which martensite or bainite particles are uniformly distributed within the fine, ferrite matrix [29]. The mechanical properties of this ferrite-bainite steel, in the as-hot-rolled condition, are attractive for the property specifications required for arctic pipeline, e.g., DBTT temperatures below - 120°C, (see fig. 17). A further advantage of this ferrite-bainite steel is that there is an abrupt increase in strength during pipe-forming due to its high work-hardening rate. This clearly demonstrates the potential use of dual-phase ferrite-bainite structures in pipeline applications.

In conclusion, from the standpoint of their superior properties, and simplicity in composition and processing, dual-phase steels show great promise, not only for the transportation industry, but for general structural applications, e.g., pipeline, wires, rods and bars. Their advantages include economy of material and enormous flexibility wherein a single alloy can be manipulated to provide a wide range of products and properties, and can be tailored to the steel plant requirements.

3. ACKNOWLEDGEMENTS

The author would like to acknowledge the graduate students, research fellows and staff of the Department of Materials Science and Mineral Engineering, University of California, Berkeley, who contributed to the alloy design programme. I am especially grateful for stimulating discussions with Professors J. W. Morris and for the collaborative work on fatigue with Prof. R. O. Ritchie. This research is supported by the Director, Office of Energy Research, Office of Basic Energy Sciences, Materials Sciences Division of the U. S. Department of Energy under Contract No. DE-AC03-76SF00098.

FIGURE CAPTIONS

Fig. 1. Schematic diagram showing conflicting properties of strength and ductility. By utilizing composite structures improved toughness without loss of strength is possible.

Fig. 2. Transmission electron microscopy showing bright field and dark field images of lath martensite and selected area diffraction patterns. Notice the austenite films surrounding martensite laths, revealed by dark field. Fe/4Cr/0.3C/2Mn alloy.

Fig. 3. Charpy toughness-tensile strength relationships of Quatough steel. QT 10 refers to a 10% Cr alloy.

Fig. 4. K_{IC} toughness - tensile strength relationships of Quatough steels compared to AISI 4340 and maraging steels.

Fig. 5. Summary of techniques used to prove extensive carbon partitioning occurs to stabilize the austenite films. Direct spectroscopic data is only currently possible via field ion atom probe analyses.

Fig. 6. Schematic representation of toughening mechanism due to retained austenite and tempered martensite embrittlement due to its decompositon to interlath carbides.

Fig. 7. Fatigue crack growth results for Quatough steels compared to AISI 4340 and 300M grades.

Fig. 8. Some wear characteristics of Quatough steel compared to some commercial wear resistant steels.

Fig. 9. Scheme showing the effects of composition on microstructure of dual phase steels. Although tensile strengths are not markedly affected, the morphology critically affect fracture and fatigue.

Fig. 10. Scheme showing heat treatment transformation paths and effects on morphology in Fe-2%Si-0.08%C steel. (ref. 23).

Fig. 11. Fatigue resistance of Fe-2Si-0.08 C dual phase steel; crack progagation rates da/dN as a function of stress intensity (ref. 23).

Fig. 12. Fatigue crack growth profiles in Fe-2%Si-0.08%C dual phase steels (ref. 23).

Fig. 13. Fatigue threshold ΔK_{TH} values for long cracks and low load ratios. Notice the superior properties of dual phase steels (ref. 23).

Fig. 14. Ductility vs. vol. fraction martensite for experimental dual phase steels.

Fig. 15. Strength vs. vol. fraction martensite for experimental dual phase steels.

Fig. 16. Cold drawing 5.5 mm rod of dual phase steel, e.g. Fe-Si-C yields high strength wire. Note that patenting heat treatments are not required as in the case of high carbon wire rods.

Fig. 17. Dual phase steel control rolling to produce plate or sheets of excellent low temperature strength and toughness, e.g. for line-pipe.

Table 1.

SOME REPRESENTATIVE MECHANICAL PROPERTIES OF Fe/Cr/Mn/C [QUATOUGH] STEELS

Alloy	Charpy Impact Energy ft/lbs.	Ultimate tensile strength ksi	Yield strength ksi	Hardness R_C +	K_{IC} ksi in.	% elongation	applications
QT 2	70-90	220	150-170	45-49	170-190	15	rounds, bars,plate mining, agricult. fasteners, etc.
QT4 Fe/4Cr/.3C/2Mn OQ	40.0	235	195	49	180.0 (calculated)	6.5	landing gear, struct. steel armored plates, pressure vessels, ordance;
QT10 Fe/10Cr/.2C/1Mn Hot rolled OQ	60.0	235	180	45	274.7 (calculated)	16.0	corrosion and wear resistant structural steel, pressure vessels. nuclear armor,etc. mining industry
OQ	46	225.5	184	47.2	-	13.5	
Hot rolled & AC	75	210.5	180	44	-	15.0	

* All properties in the quench and 200°C temper (1 hour) condition.

OQ oil quench
AC air cool

** Alloy refers to Cr content; thus QT2 = 2wt% Cr, etc.

+ Hardness principally depends on carbon content; range 0.24-0.3wt%

Table II

CORROSION* DATA FOR LOW CARBON QUA-TOUGH AND AND SOME COMMERCIAL STEELS

Specimen	Condition	Weight Loss Mg/Decimeter^2	MmPY Mm Per Year
Fe-2Si-0.1C	As-received	2091.6	1.70
	Duplex Ferrite-Martensite	1956.4	1.59
AISI 1010	As-received	2077.2	1.68
	Duplex Ferrite-Martensite	1946.9	1.58
Fe-4Cr-0.3C-2Mn	As-quenched	1173.5	0.95
	200°C Tempered	988.5	0.80
Fe-4Cr-0.3C-5Ni	As-quenched (Coarse grained	926.1	0.75
	As-quenched (Grain refined)	774.5	0.63
AISI 4340	As-received	--	2.79.
AISI 410 (Stainless steel)	As-received	--	3.05

*15% NaCl, 100 ppm CO_2 (pH 4.4) at 250°C (Courtesy of Battelle Northwest and R. Clark).

REFERENCES

1. B.V.N. Rao and G. Thomas, Metall. Trans. 11A, (1980), 441.
2. G. Thomas, Fundamental Aspects of Structural Alloy Design, R.I. Jaffee and B.A. Wilcox, eds. Plenum Press, New York, (1977), 331.
3. G. Thomas, J. Iron and Steel, 46, (1973), 451.
4. G. Thomas, Design of Strong, Ductile, Duplex Low Alloy Steels, N. R. Comins and J. B. Clark, eds. Conf. Proc. on Specialty Steels and Hard Materials, Pretoria, S. Africa, (1983), 55.
5. G. Thomas, Metall. Trans, 9A, (1978), 439.
6. A. Jhingan, M. Sarikaya, and G. Thomas, Metall. Trans. 14A,(1983), 1121.
7. G. Thomas, M. Sarikaya, S. J. Barnard and G.D.W. Smith, Advances in Physical Metallurgy of Steels, Inst. of Metals, London, (1983), 259.
8. K. Easterling and A.R. Tholen, Acta. Metall., 28, (1980), 1229.
9. W. J. Salesky, R. M. Fisher, G. Thomas and R. O. Ritchie, Wear of Material, (ASME), (1983), 434.
10. C. K. Kwok and G. Thomas, ibid, 140.
11. C. K. Kwok and G. Thomas, ibid, 612.
12. A. T. Davenport, ed. Formable HSLA and Dual-Phase Steels, A.I.M.E., New York, New York. (1979).
13. R.A. Kot, J. W. Morris, Jr., eds. Structure and Properties of Dual-Phase Steels, A.I.M.E., New York, New York, (1979).
14. R.A. Kot, B.L. Bramfitt, eds., Fundamentals of Dual-Phase Steel, A.I.E., New York, New York, (1981).
15. J. Y. Koo and G. Thomas, Metall. Trans. 8A, (1977), 525.

16. M. A. Meyers, O. T. Inal, eds., Elsevier Science Pub. G. Thomas, Frontiers in Materials Tech. Ch. 3, (1985), 89.

17. N. J. Kim and G. Thomas, Metall. Trans. 12A, (1981), 483.

18. J. A. Wazynczuk, R. O. Ritchie, and G. Thomas, Mat. Sci. and Engin. 62, (1984), 79.

19. S. D. Antolovitch, R. O. Ritchie, and W. W. Gerberich, eds. Mech. Properties and Phase Transformation in Engineering Materials, TMS-AIME pubs. (1986), 59.

20. R. O. Ritchie, Int. Met. Rev. 20, (1979), 205.

21. E. Zaiken and R. O. Ritchie, Mater. Sci and Engin. 70, (1985), 151.

22. J-L. Tzou and R. O. Ritchie, Scripta Met. 19, (1985), 751.

23. V.B. Dutta, R. Suresh, R. O. Ritchie and G. Thomas, Fracture Prevention in Energy and Transport Systems, I. Le May and S.N. Monteiro, eds. EMAS, U.K., (1983), 457.

24. G. Thomas, and J. Y. Koo, Structure and Properties of Dual-Phase Steels, A.I.M.E., New York, (1979), 183.

25. R. H. Hoel and G. Thomas, Scripta Metall., 15, (1981), 867.

26. A. Nakagawa and G. Thomas, Metall. Trans, 16A, (1985), 831.

27. G. Thomas and J. A. Ahn, "Interwire 85", 55 Int. Conf. (1985), 55.

28. G. Thomas, Mechanical Properties and Phase Transformation in Engineering Materials, S. D. Antolovitch, R. O. Ritchie, and W. W. Gerberich, eds. TMS-AIME pubs. (1986), 147.

29. N. J. Kim and G. Thomas, Mat. Sci. & Tech. 1 (1985), 32.

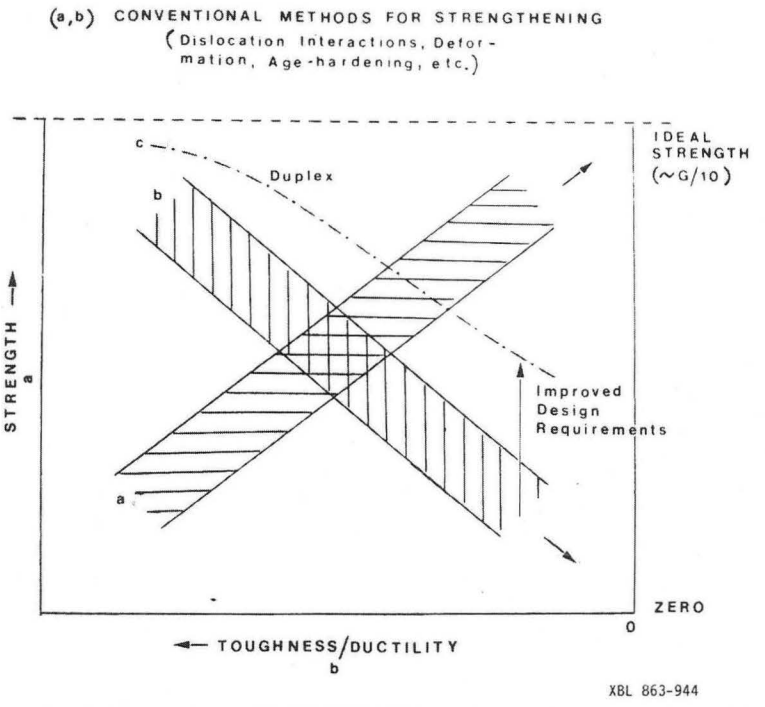

Fig. 1

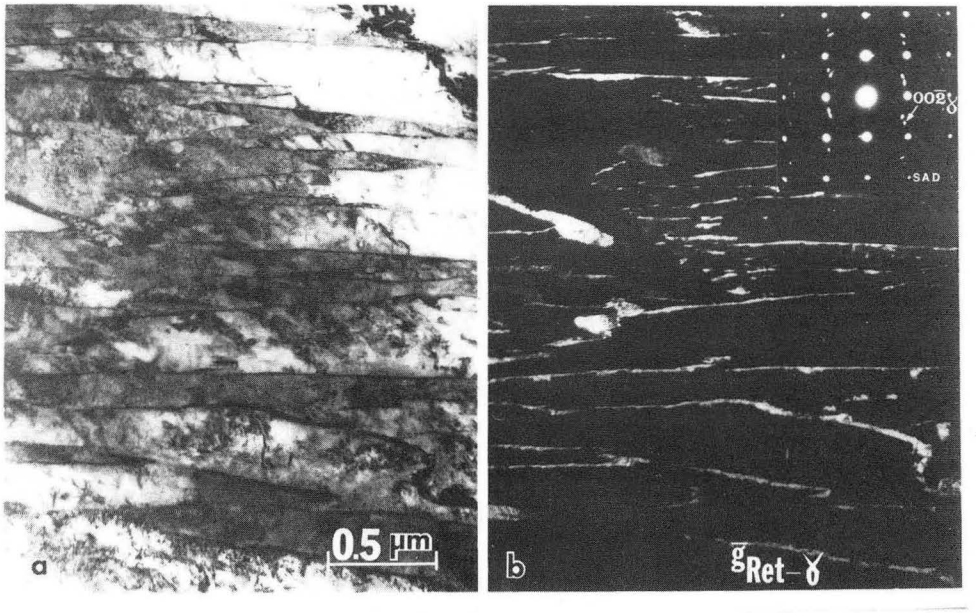

XBB 817-7032

Fig. 2

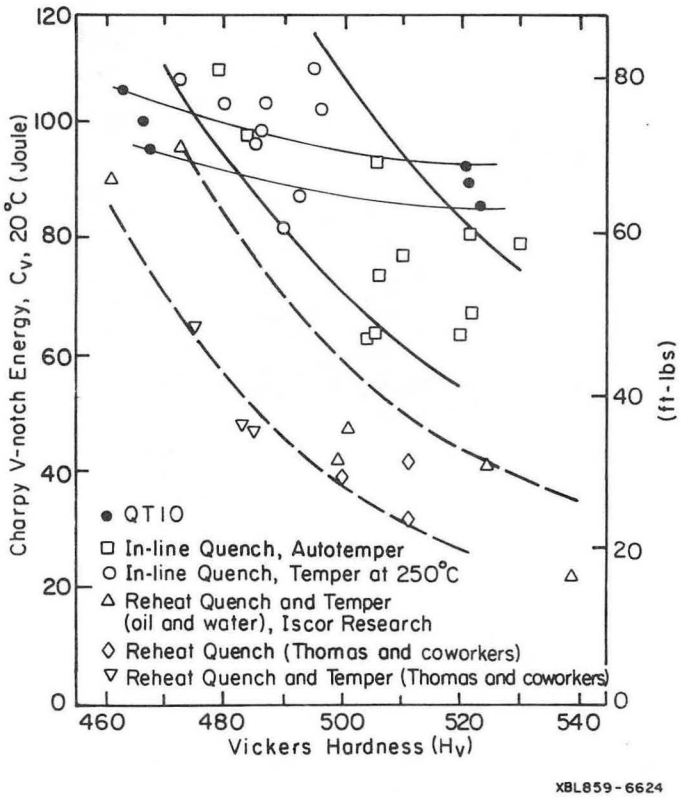
Charpy V-notch Energy, C_v, 20°C (Joule)
(ft-lbs)
Vickers Hardness (H_V)
120
100
80
60
40
20
0
460
480
500
520
540
● QT10
□ In-line Quench, Autotemper
○ In-line Quench, Temper at 250°C
△ Reheat Quench and Temper (oil and water), Iscor Research
◇ Reheat Quench (Thomas and coworkers)
▽ Reheat Quench and Temper (Thomas and coworkers)
XBL859-6624

Fig. 3

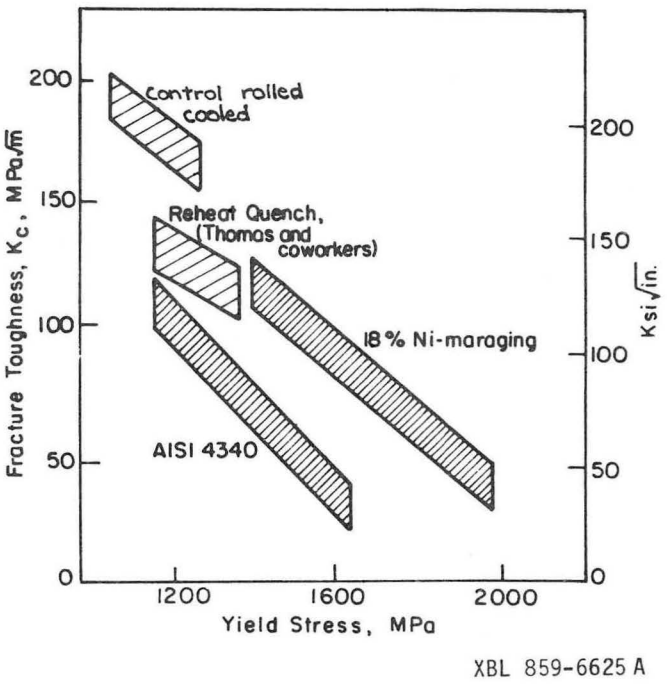
Fracture Toughness, K_c, MPa$\sqrt{m}$
Ksi$\sqrt{in.}$
Yield Stress, MPa
200
150
100
50
0
1200
1600
2000
Control rolled cooled
Reheat Quench, (Thomas and coworkers)
18% Ni-maraging
AISI 4340
XBL 859-6625 A

Fig. 4

CARBON PARTITIONING IN RETAINED-AUSTENITE IN LATH-MARTENSITIC STEELS

TRANSMISSION ELECTRON MICROSCOPE - IMAGE STUDIES

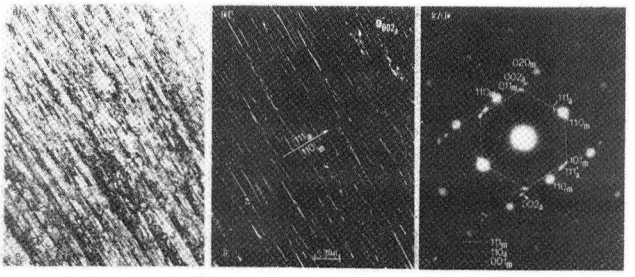

FIGURE 1 - (a) BF and (b) DF $\{00\bar{2}_\gamma\}$ images illustrating the general appearance of thin films of Ret-γ at the martensite lath boundaries (0.5 at.% C steel). (c) Composite SAD pattern of martensite (m) and austenite (a).

The microstructure consists of dislocated lath martensite with fairly straignt boundaries and thin film Ret-γ at the lath-like martensite crystal boundaries. DF micrographs (fig. 1) shows an extensive amount of Ret-γ (5 vol.%) even at this low carbon level. The existence of this high temperature phase at low temperatures is attributed to several mechanisms in which interstitial C stabilizes the austenite. (i) Chemical stabilization: Diffusion and partitioning of C in Ret-γ decrease the local M_s temperature and inhibit further transformation. (ii) Thermal stabilization: During quenching interstitial C forms dislocation atmospheres in α' and at the α'/γ interface, pinning the dislocations and suppressing interface motion. (iii) Mechanical stabilization: Part of the austenite to martensite shear transformation strains is accommodated by soft γ which deforms extensively to prohibit the transformation.

The average C concentration in Ret-γ can be determined by measurements of shift in positions of the holz lines in CBED patterns in relation to the change in the lattice parameter of the Ret-γ, due to C: $(\Delta a_\gamma/a_{ref}) = (2/3)[(p_\gamma/q_\gamma) - (p_{ref}/q_{ref})](8/115)^{\frac{1}{2}}$. Ni (99.99% with a_o = 3.5238) was used as a reference, and results cross-checked with Cu (99.999% with a_o = 3.6150). For the example shown in fig. 2, C at.% = 4.9 ± 0.6 (at.% C alloy = 0.7) taking $a_{Ret\text{-}\gamma}$ = 3.555 + 0.044X (w/o C).

Retained austenite (Ret-γ) has been identified in a number of carbon containing lath martensitic steels with M_s and M_f temperatures well above room temperature. Because of its beneficial effects on the mechanical properties (especially fracture toughness) of HSLA steels the influence of interstitial C in stabilizing the γ has been studied in detail using TEM, CBED and FIM-APA techniques.

Steels were austenitized at 1100°C, and oil quenched. TEM foils were prepared by electropolishing in chromacetic at room temperature (RT), and Cu and Ni standards in 25% NHO_3 in CH_3-OH at -30°C. Some steel foils were etched for CBED by "dipping" in 15% $HClO_4$-5% $C_3H_5(OH)_3$-CH_3COOH at -25°C. FIM tips were electropolished in 25% $HClO_4$ in CH_3-COOH at RT.

CONVERGENT BEAM ELECTRON DIFFRACTION

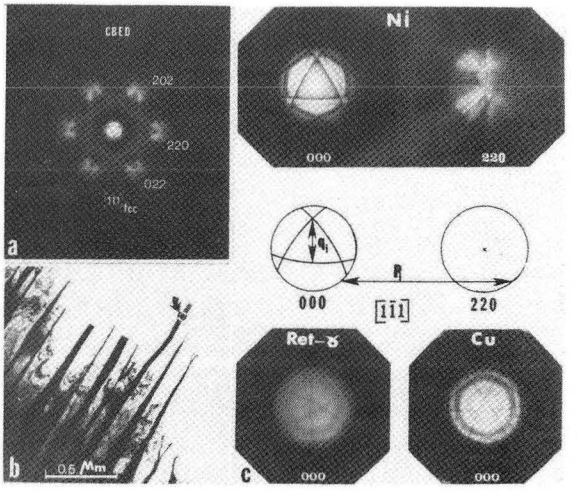

FIGURE 2 - (a) Nickel (fcc) 111 CBED-pattern at 100 kV reveals trigonal symmetry. (b) BF image, from a specially prepared foil, shows the Ret-γ films extending into the perforation. (c) Discs formed by forward scattered beams from Ni, Ret-γ, and Cu (note q_i and P_i).

FIELD ION MICROSCOPY - ATOM PROBE ANALYSIS

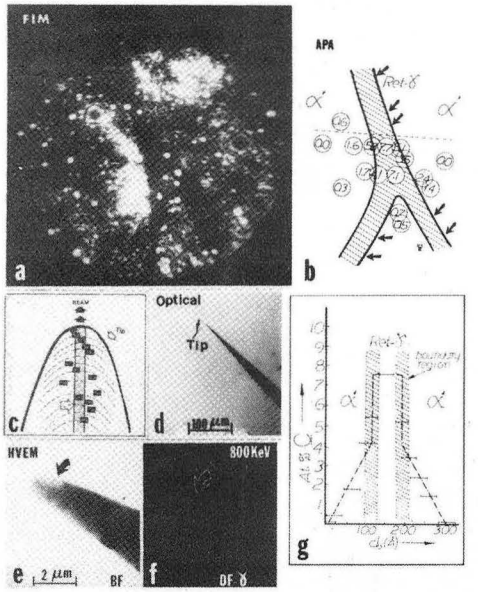

FIGURE 3 - (a) FIM image of Ret-γ. (b) Regions of APA analysis. (c) Illustration of the analysis of subsurface regions by field evaporation. (d) Low magnification image of the tip. (e) HVEM BF and (f) DF images reveal Ret-γ. (h) Concentration profile for C across the interface.

Atom Probe analysis provided direct quantitative determination of the C distribution in α' and Ret-γ at 20-30 Å resolution. Considerable C enrichment occurs in Ret-γ - direct evidence of chemical stabilization (figs. 3-4). Detailed measurements of C distribution in a thicker Ret-γ film (fig. 4) gave an average concentration of 3.0 at.% and up to 8.5 at.% at the α'/Ret-γ interface (Thermal stabilization). The extent of deformation (Mechanical stabilization) is discernible in TEM micrographs in fig. 4. There is no apparent change in distribution of substitutional alloying elements (Cr and Mn, fig. 4) in α' and Ret-γ. Hence changes in the amount of Ret-γ with alloying elements are attributed to their interaction with C influencing its mobility. Thus the overall stability of thin film Ret-γ is due to effects of several mechanisms.

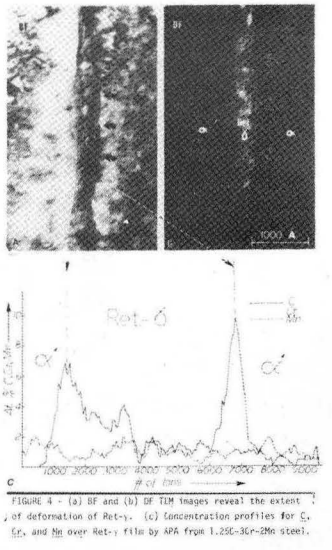

FIGURE 4 - (a) BF and (b) DF TEM images reveal the extent of deformation of Ret-γ. (c) Concentration profiles for C, Cr, and Mn over Ret-γ film by APA from 1.25C-3Cr-2Mn steel.

XBB 817-7029

Fig. 5

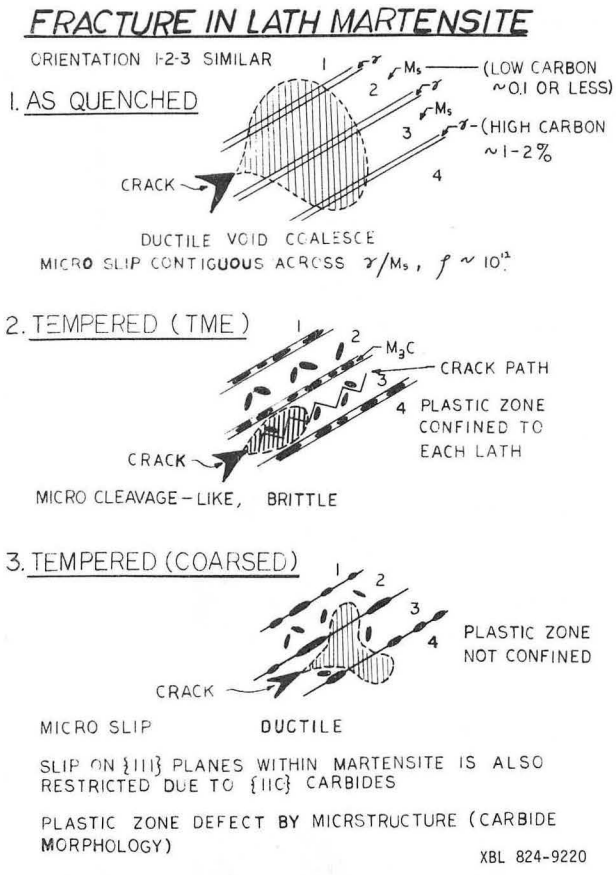

Fig. 6

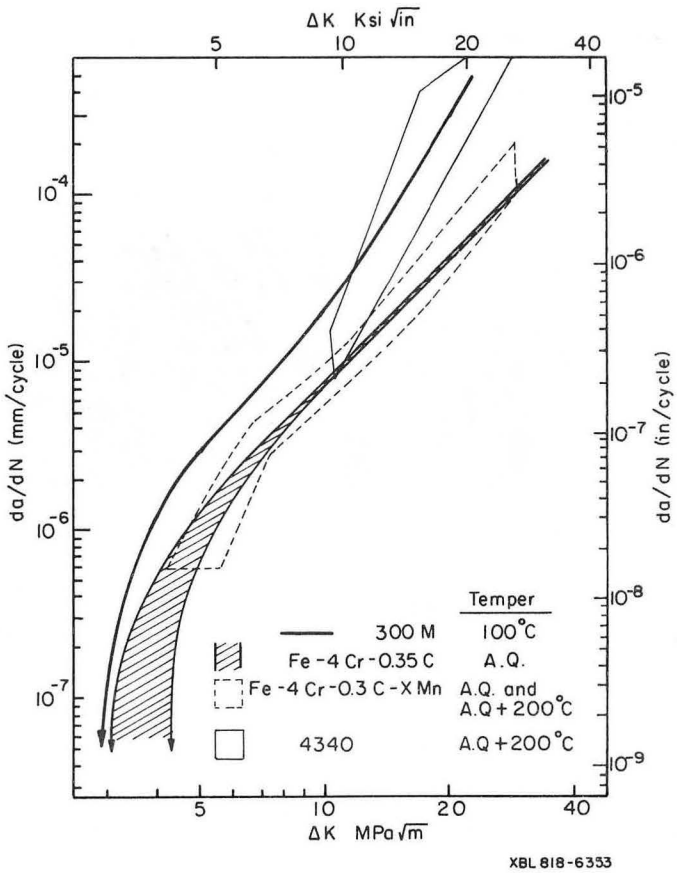

Fig. 7

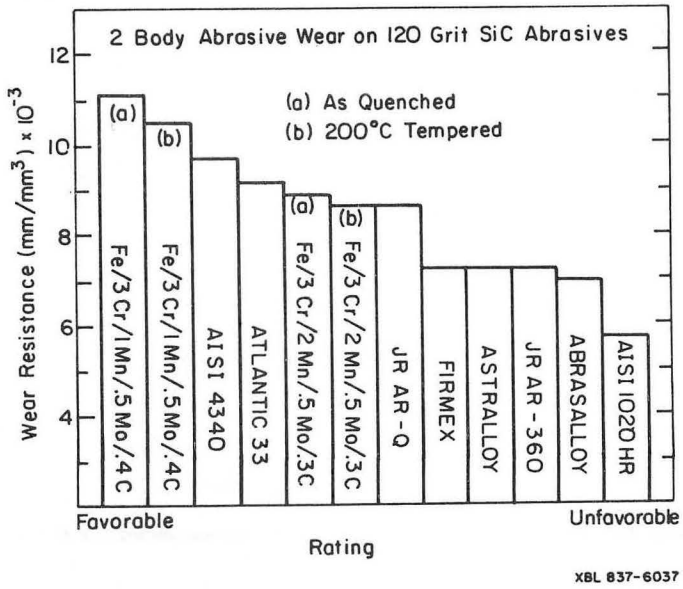

Fig. 8

DUPLEX FERRITE/MARTENSITE STRUCTURES DEVELOPED IN Fe/0.1C/X ALLOYS

OPTICAL MICROGRAPH

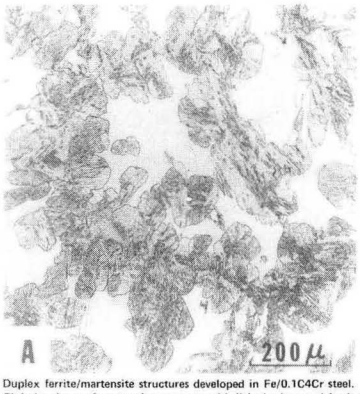

Duplex ferrite/martensite structures developed in Fe/0.1C4Cr steel. Globular shape of martensite contrasts with light background ferrite.

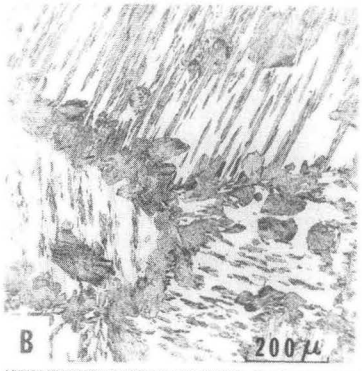

Duplex structures developed in Fe/0.1C/0.5Cr steel. Predominantly needle-like martensite is shown within each prior austenite grain. Prior austenite grain boundaries are decorated with continuous martensite phase.

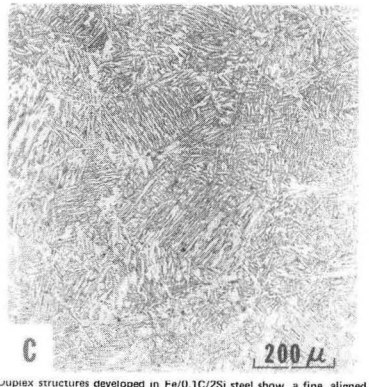

Duplex structures developed in Fe/0.1C/2Si steel show a fine, aligned, and acicular shape of martensite within each prior austenite grain.

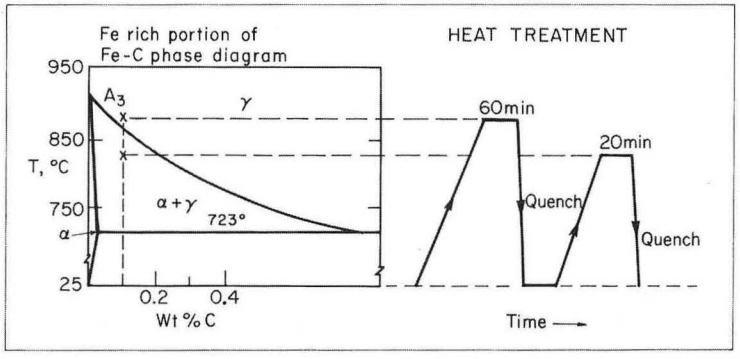

MECHANICAL PROPERTIES

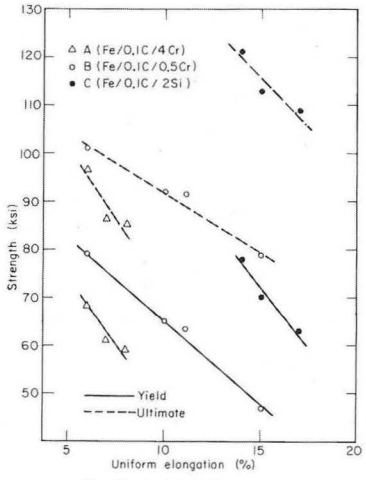

Depending on the annealing temperature in the $(\alpha + \gamma)$ range, various volume fraction of martensite and a wide range of strength and elongation combinations are obtained.

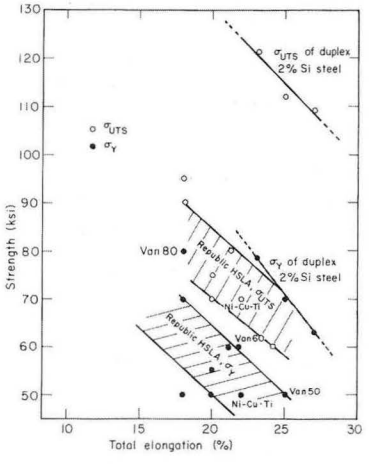

Tensile properties of the duplex 2% Si steel are compared with those of commercial HSLA steels.

The incorporation of the strong phase martensite as a load carrying constituent in a ductile ferrite matrix can strengthen the composite alloy. The production of such duplex ferrite/martensite structures in Fe/0.1C/X alloys (X being a small amount of a substitutional alloying element) is carried out by an initial austenitizing treatment followed by annealing in the $(\alpha + \gamma)$ with intermediate quenching. Depending on X and the exact heat treatment, various morphologies and shapes of martensite in the ferrite matrix are obtained (Figs. A, B and C) and these seriously affect the corresponding mechanical properties.

A globular shape of the second phase martensite, combined with continuous martensite along the prior austenite grain boundaries (Fig. A), results in relatively poor tensile properties. With microstructures containing a combination of needle-like martensite within each prior austenite grain (Fig. B), while still showing continuous globular martensite along the prior austenite grain boundaries, somewhat improved tensile properties are exhibited. However, upon obtaining a complete needle-like martensite (Fig. C) a superior strength and elongation-ductility combination is found (these properties are compared with these of commercial HSLA steels).

Other factors, such as carbide morphology, solid solution strengthening, etc. were not found to be as significant in determining mechanical properties as the shape and distribution of the martensite phase. Photos were made with polaroid film at 130 ×; 2% nital etch.

XBB 866-5888

Fig. 9

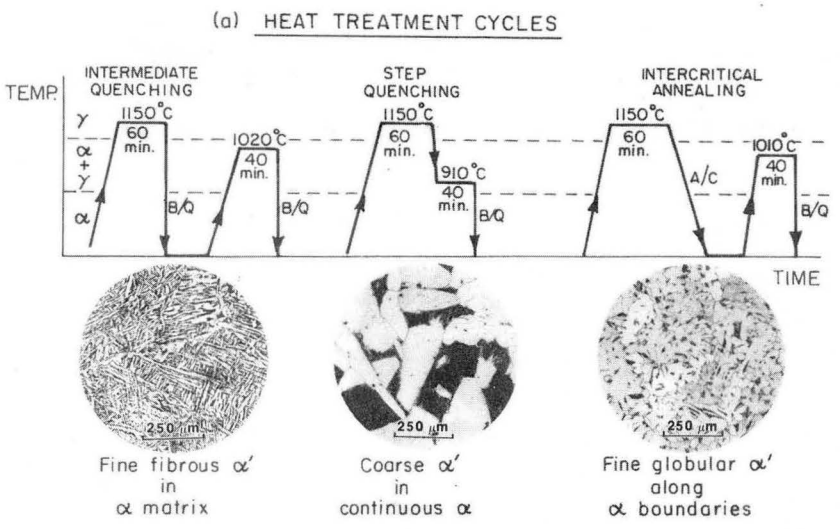

XBB 833-2300

Fig. 10

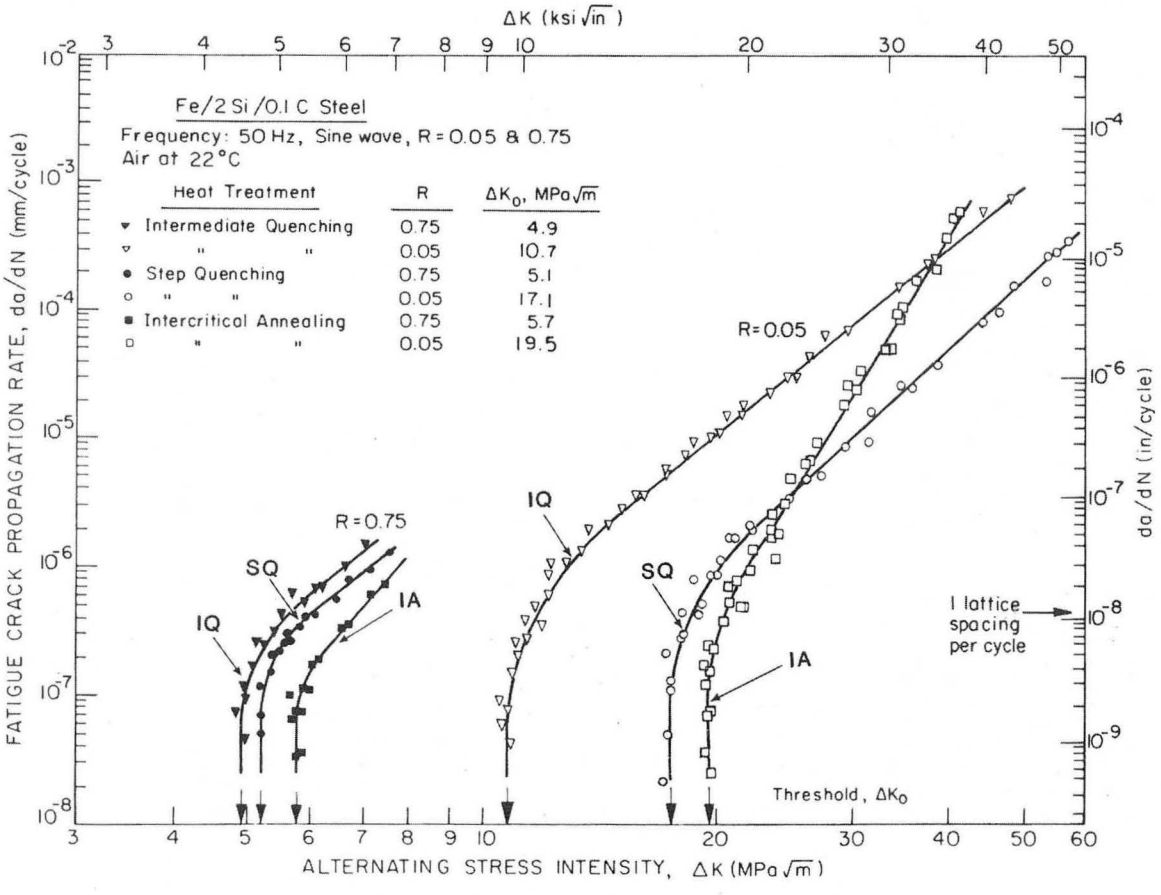

XBL 838-10897

Fig. 11

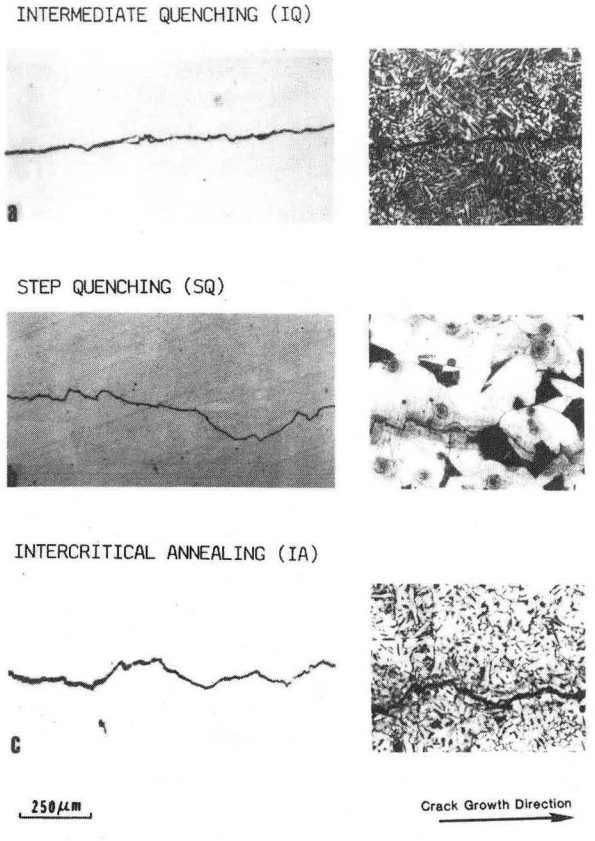

XBB 839-7928

Fig. 12

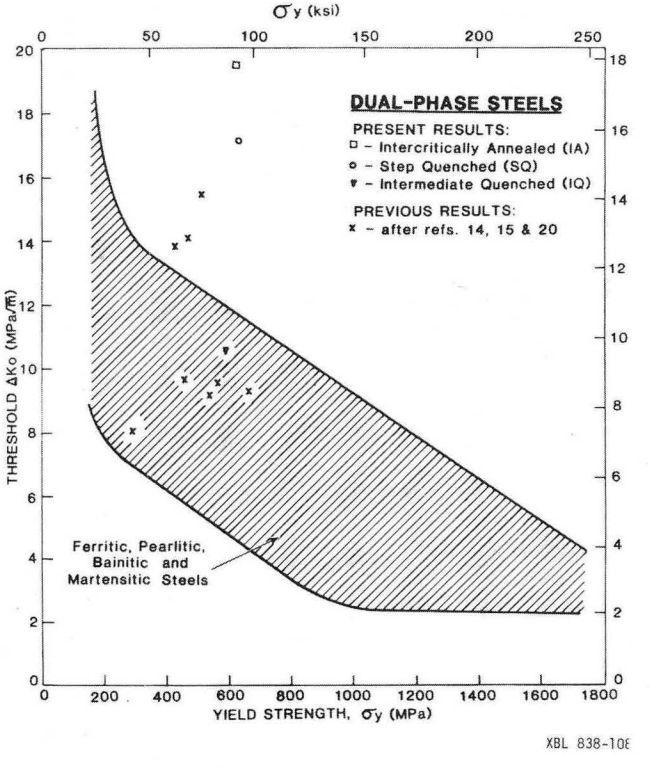

XBL 838-10

Fig. 13

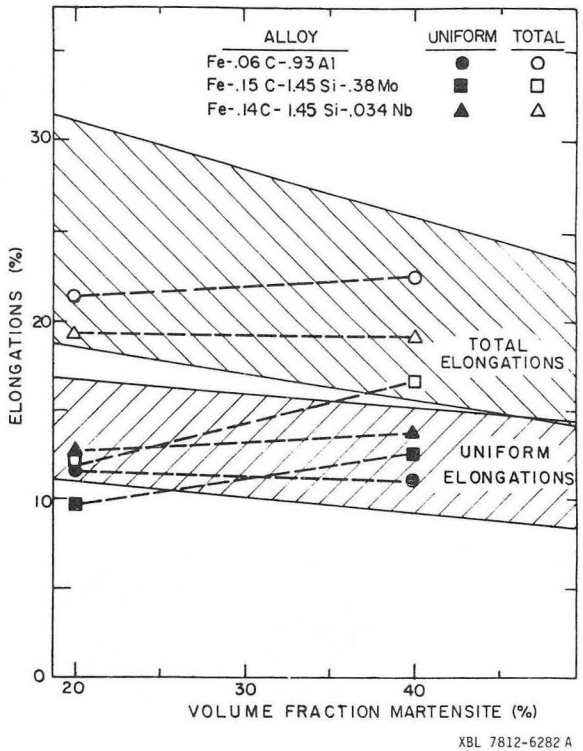
ALLOY
UNIFORM
TOTAL
Fe-.06 C-.93 Al
Fe-.15 C-1.45 Si-.38 Mo
Fe-.14 C- 1.45 Si-.034 Nb
TOTAL ELONGATIONS
UNIFORM ELONGATIONS
ELONGATIONS (%)
VOLUME FRACTION MARTENSITE (%)
XBL 7812-6282 A

Fig. 14

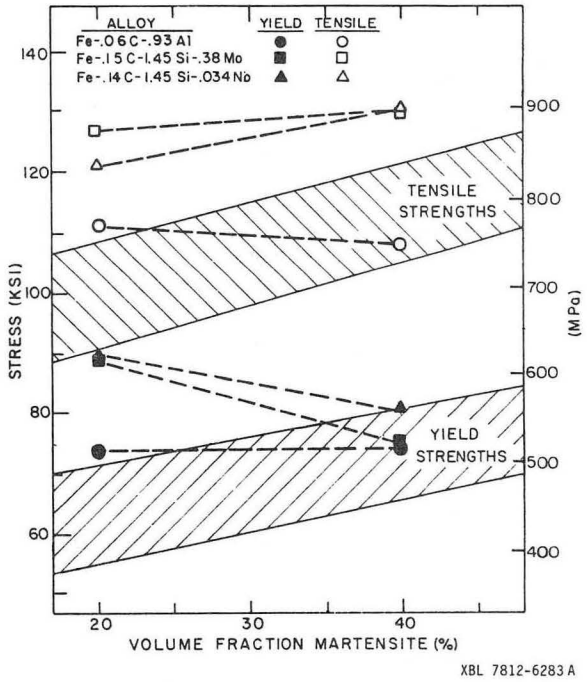
ALLOY
YIELD
TENSILE
Fe-.06 C-.93 Al
Fe-.15 C-1.45 Si-.38 Mo
Fe-.14 C-1.45 Si-.034 Nb
TENSILE STRENGTHS
YIELD STRENGTHS
STRESS (KSI)
(MPa)
VOLUME FRACTION MARTENSITE (%)
XBL 7812-6283 A

Fig. 15

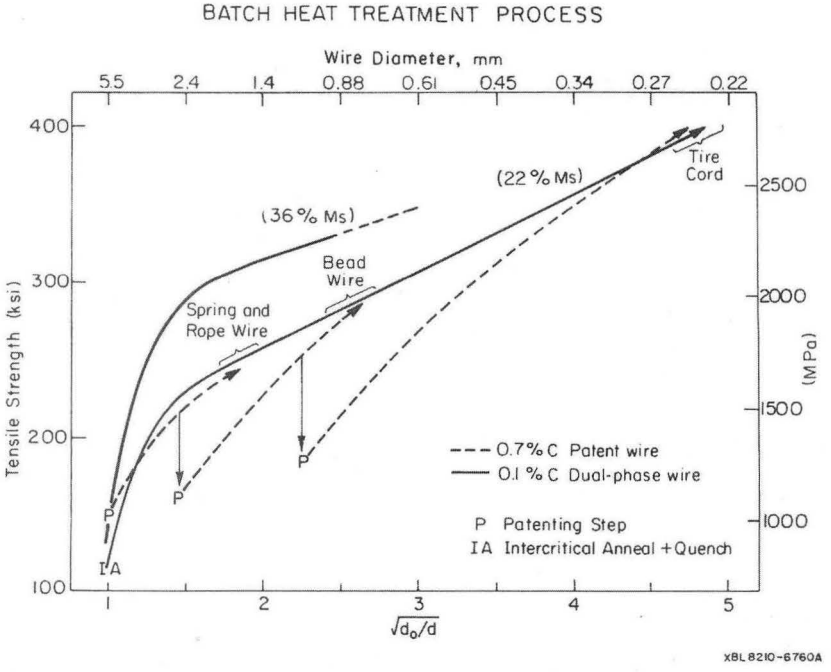

Fig. 16

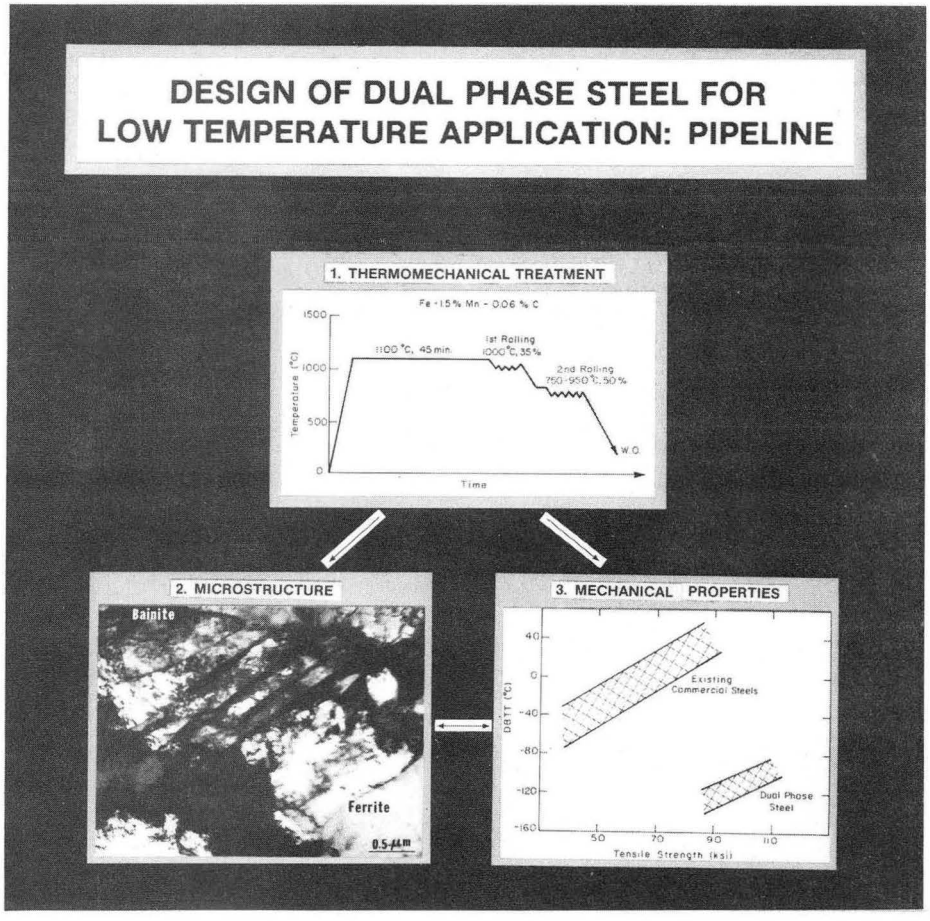

XBB 810-10828

Fig. 17

LAWRENCE BERKELEY LABORATORY
TECHNICAL INFORMATION DEPARTMENT
UNIVERSITY OF CALIFORNIA
BERKELEY, CALIFORNIA 94720